Sudden Unison: Quantitative Analysis of Chimera State Collapse and Epileptic Seizures

Henry Mitchell[1,2], Chris Danforth[1,4], and Matt Mahoney[3,4]

[1]Department of Mathematics and Statistics, University of Vermont College of Engineering and Mathematical Sciences
[2]Department of Physics, University of Vermont College of Arts and Sciences
[3]Department of Neurology, University of Vermont Larner College of Medicince
[4]Department of Computer Science, University of Vermont College of Engineering and Mathematical Sciences

March 27, 2019

Abstract

Contents

Chapter 1

Introduction

Pick bet ter title

As this work is an analysis of the relationship between chimera states and seizures, it is important to develop a baseline understanding of what each of those are.

1.1 Chimera States

Italicize terms.

Put this in bibte

The science and mathematics of synchronization are among history's most well-studied areas of research. One of the earliest well-documented appearances of synchrony in unexpected places was observed in 1665 by Dutch physicist Christiaan Huygens, the inventor of the pendulum clock. He noticed that two clocks hung from the same beam would eventually synchronize with each other. He supposed that this was due to minuscule energy transfers between the two clocks through the wooden beam. This hypothesis was proven nearly 350 years later which shows that even the simplest-seeming synchronization behavior results from complex dynamics [20].

This behavior extends to larger systems that two clocks. A classic demonstration in many classes on the mathematics of synchronization depicts the same phenomenon with more oscillators [19]. One places a platform on top of a set of rollers, and places at least two metronomes on that platform (see fig. 1.1 for a drawing). When these metronomes are started with the same frequency, out of phase with each other, over time their phases drift until they synchronize.

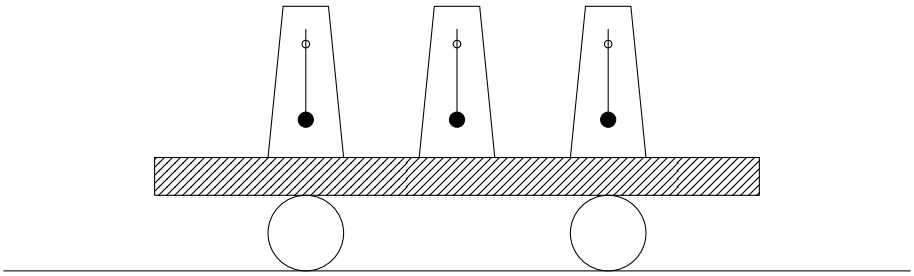

Figure 1.1: The classic demonstration of Huygens synchronization. When the metronomes are set running, they eventualy synchronize due to the light coupling provided by the platform's ability to roll.

One example of more complex behavior arising from similar mechanisms is the coexistence of synchrony and asynchrony within a system of identical coupled oscillators, a phenomenon known as a *chimera state* [1, 14]. The existence of these chimera states are surprising, as they represent asymmetry within symmetric systems. The first time this behavior was observed was in a ring of *nonlocally coupled* oscillators [14]. While global coupling is an all-to-all interaction and local

coupling is a nearest-neighbor interaction, nonlocal coupling is a mixture of the two. The model is expressible in one dimension as

$$\frac{\partial}{\partial t}A(x,t) = (1+i\omega_0)A - (1+ib)|A|^2 A + K(1+ia)(Z(x,t) - A(x,t)) \tag{1.1}$$

where

$$Z(x,t) = \int G(x-x')A(x',t)\,\mathrm{d}x' \quad \text{and} \quad G(y) = \frac{\kappa}{2}e^{-k|y|}, \tag{1.2}$$

which reduces to the phase equation

$$\frac{\partial}{\partial t}\phi(x,t) = \omega - \int G(x-x')\sin(\phi(x,t) - \phi(x',t) + \alpha)\,\mathrm{d}x' \quad \text{where} \quad \tan(\alpha) = \frac{b-a}{1+ab}. \tag{1.3}$$

When numerically simulated using a discrete approximation, this system quickly falls into a chimera state (fig. 1.2).

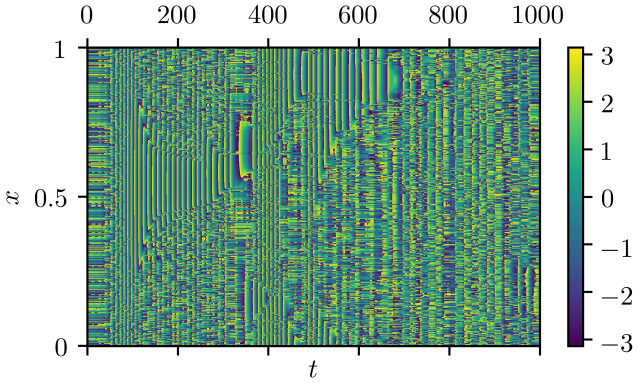

(a) The time series of the Kuramoto simulation.

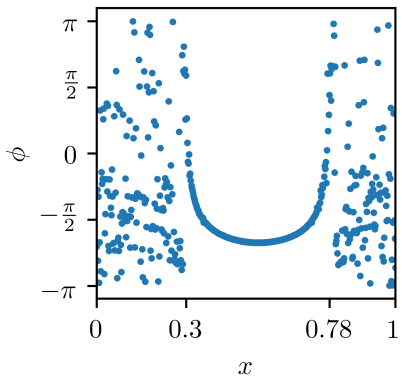

(b) A snapshot at $t = 120$.

Figure 1.2: The results of a simulation of a Kuramoto oscillator, as described in eq. (1.3). A 4th-order Runge-Kutta solver ($\mathrm{d}t = 0.01$, $t_{\max} = 1000$) was run on a system of 512 oscillators. Figure 1.2a shows the entire time series of the simulation. The behavior represented there is quite complex, with several distinct qualitative changes to the patterns in the system. However, in-depth analysis of this system is beyond the purview of this work. Figure 1.2b shows a snapshot of the state of the system at $t =$. Note the juxtaposition of asynchronous ($0 \lesssim x \lesssim 0.3$ and $0.78 \lesssim x \lesssim 1$) and synchronous (oscillators $0.3 \lesssim x \lesssim 0.78$).

Since then, chimera states have been found in simpler systems still. One of the simplest is the Abrams model, two populations of identical oscillators with a stronger coupling strength within the populations than between them [2]. The equation describing this system is given as

$$\frac{\mathrm{d}\theta_i^\sigma}{\mathrm{d}t} = \omega + \sum_{\sigma'=1}^{2}\frac{K_{\sigma\sigma'}}{N_{\sigma'}}\sum_{j=1}^{N_{\sigma'}}\sin\left(\theta_j^{\sigma'} - \theta_i^\sigma - \alpha\right) \quad \text{where} \quad K = \begin{bmatrix}\mu & \nu \\ \nu & \mu\end{bmatrix} \quad \text{and} \quad \sigma \in \{1,2\}. \tag{1.4}$$

In this model, μ represents the intra-population strength, and ν represents the inter-population strength, meaning $\mu > \nu$. Time can be scaled such that $\mu + \nu = 1$. If $\mu - \nu$ is not too large, and α is not too much less than $\frac{\pi}{2}$, then this system can produce chimera states.

Insert pictures

A similar system was also analyzed in the physical world [17]. Two swinging platforms were coupled together with springs of variable spring constant κ, and 15 metronomes—all tuned to the same frequency—were placed on each platform. For a wide range of values of κ, all of the metronomes on one platform would synchronize, while the metronomes on other platform would remain asynchronous. This system is directly analogous to the Abrams model. The metronomes on the same platform are coupled through the motion of the swing, which heavily influences the motion of the metronomes. This intra-community coupling is represented by μ in the Abrams model. The metronomes on opposite platforms are coupled through the springs, which is a much weaker interaction, represented in the Abrams model by ν.

While chimera states my present themselves obviously when observed in a plot or the physical world, they can be harder to pin down analytically. One useful pair of measures for the presence of a chimera state are the *chimera-like index* χ and the *metastability index* m [10, 23]. We will investigate a system of M communities of nonlocally-coupled oscillators, and we sample their phases at times $t \in [1, \ldots, T]$. In order to develop these two measures, one must first develop the *order parameter* $\phi(t) = \left|\left\langle e^{i\theta_k(t)}\right\rangle_{k\in C}\right|$, where θ is the phase of oscillator k, and $\langle f\rangle_{k\in c}$ is the average of f over all k in community C. ϕ indicates the instantaneous synchrony of a community (how similar the phases of the oscillators are to the others in C), and not its overall coherence (how similar the trajectories of the oscillators are). From this, we find the two measures:

$$m = \langle \sigma_{\text{met}} \rangle_C \qquad \text{where} \quad \sigma_{\text{met}}(c) = \frac{1}{T-1}\sum_{t\le T} \phi_c(t) - \langle \phi_c \rangle_T{}^2 \tag{1.5}$$

$$\chi = \langle \sigma_{\text{chi}} \rangle_T \qquad \text{where} \quad \sigma_{\text{chi}}(t) = \frac{1}{M-1}\sum_{c\in C} \phi_c(t) - \langle \phi_c \rangle_C{}^2 \tag{1.6}$$

To put this into words, the metastability index is the average across communities of the variance of the order parameter within a given community over time, while the chimera-like index is the average over time of the variance of the order parameter across communities.

This gives us some maximum possible values for these measures [23]. If a community c spends equal time in all stages of synchronization (i.e., the phase parameter of c is uniformly distributed), then $\sigma_{\text{met}}(c)$ is at its maximum, the variance of the uniform distribution: $m_{\max} = \frac{1}{12}$. If a community spends equal time in a maximally chimeric state and a minimally chimeric state, then its chimera-like index will be at its maximum[1]: $\chi_{\max} = \frac{1}{7}$. Therefore, when the normalized chimera-like and metastability indices are presented, they will be presented normalized to $\frac{1}{7}$ and $\frac{1}{12}$, respectively.

Chimera states have been observed in many other systems, whether they be purely mathematical, biological, electrical, or mechanical [1, 3, 10, 13, 14, 17, 18, 21–23, 28]. Find a transition.

1.2 Seizures

1.2.1 Neuroanatomy and Neurophysiology

Since the brain is an electrochemical device, its function and disorders are often best talked about from an electrical standpoint [7]. *Neurons* are cells which are specialized for communication (see fig. 1.3 for a diagram). They receive input signals through *synapses* at the ends of their *dendrites*, Cite

[1] While it is possible for half of a system's communities to be synchronous and the other half asynchronous for all times (resulting in a chimera-like index of $\frac{2}{7}$), this is transient due to the effects of metastability [23]. Therefore, we will ignore this case.

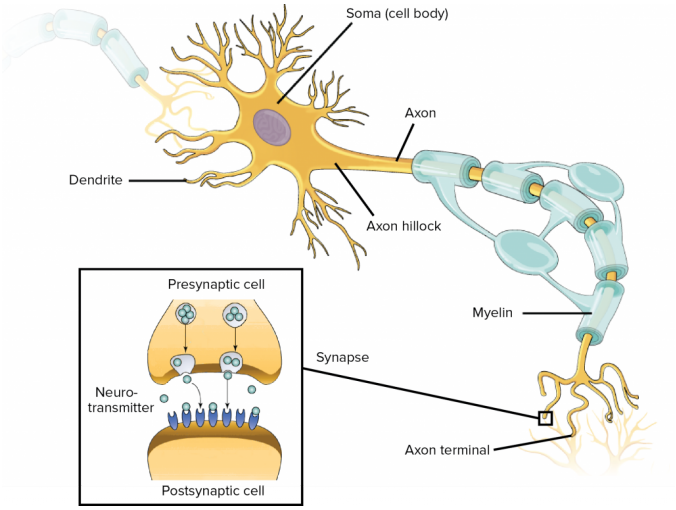

Figure 1.3: A diagram of the anatomy of a neuron.

branches in their large tree of inputs. The trunk of the dendritic tree is the *soma*, the cell body. If the sum signal entering the soma from all of the dendrites is sufficient, the neuron *fires*, sending a signal to its outputs.

When a neuron fires, it sends an electrochemical signal down its *axon*—its long stem—to the output synapses at its *axon terminals*. This signal is known as an *action potential*. The action potential is discrete; a neuron sends the same signal any time its input threshold is surpassed, no matter how far above the threshold the input is. It is the propagation along the axon of a potential difference across the cell membrane of the neuron. This potential difference is created by different concentrations of various ions in and out of the cell, controlled by pumps (which push Na^+ out of the cell and draw K^+ into it) and gates (which allow the ion concentrations to equilibrate). It is important to note that processes involving Na^+ are faster than those involving K^+. Each location along the axon goes through the following six stages, in total taking approximately 1 ms:

Equilibrium No current flows through the membrane, which has a potential of $-75\,\text{mV}$ across it[2].

Depolarization The potential difference propagating from upstream in the axon activates ion channel gates, allowing Na^+ to flow into the axon, countered by the K^+ flowing out.

Amplification Because the K^+ processes are slower than the Na^+ processes, if the incoming signal is strong enough, the influx of Na^+ is too fast for the outflow of K^+ to compensate. This results in a positive feedback loop, wherein the Na^+ flowing in increases the membrane potential, which increases the rate at which Na^+ flows into the neuron, which continues to feed itself.

Repolarization When the Na^+ channels are fully open, the K^+ channels are finally able to compensate for the influx.

Hyper-polarization The Na^+ channels close, and the slower K^+ channels remain open. This causes more K^+ to flow out of the cell than Na^+ flowed in, dropping the potential below its equilibrium state.

Refractory Period The Na^+ channels are briefly unable to open, which means that neurons need a brief time to "recharge" after an action potential.

[2]All potentials hold the extracellular matrix at 0 V. In other words, the interior of the cell is at a lower potential than the exterior.

Micro-scale models

All of these processes are summarized in the *Hodgkin-Huxley model*[3] describing the membrane potential U:

$$C_m\dot{U} + p_{A\mathrm{K}^+}\bar{g}_{A\mathrm{K}^+}(U - E_{\mathrm{K}^+}) + p_{A\mathrm{Na}^+}\bar{g}_{A\mathrm{Na}^+}(U - E_{\mathrm{Na}^+}) + g_l(U - E_l) = I_m \tag{1.7}$$

where

$$\begin{aligned} \dot{n} &= \alpha_n(1-n)\beta_n n \\ \dot{m} &= \alpha_m(1-m)\beta_m m \quad \text{and} \quad \begin{aligned} p_{A\mathrm{K}^+} &= n^4 \\ p_{A\mathrm{Na}^+} &= m^3 h \end{aligned} \\ \dot{h} &= \alpha_h(1-h)\beta_h h \end{aligned} \tag{1.8}$$

where g_i is the conductance of the membrane to ion i, p_{Ai} is the proportion of i-gates which are open (developed from a Markov model with transition rates α and β), E_i is the equilibrium potential of ion i, C_m is the capacitance of the membrane, and I_m is an external current (the tuned input parameter). This model is highly accurate, and won its developers a Nobel Prize in Physiology or Medicine. Many bifurcation analyses have been performed on these equations, and they are well understood [9].

However, the Hodgkin-Huxley model is not particularly useful for large-scale brain simulation. Given that most behavior of the brain is emergent[4], it is important to understand neurons' interactions. As is often the case with emergent phenomena, it is wildly impractical to simulate the collective behavior of a brain by simulating its constituent neurons. Since the human brain has approximately 10^{11} neurons with 10^{14} synapses, direct simulation is too computationally intensive. In order to better understand the dynamics of large portions of the brain, many researchers turned to the techniques of thermal and statistical physics [6]. Particularly, *neural ensemble models* and *neural mass models* are popular approaches to studying brain behavior.

Meso-scale Models

Neural ensemble models treat patches of the brain as a collective group, taking into account neurons' mean activity, as well as their variance. They assume that the firings of the neurons within a group are sufficiently uncorrelated to result in a Gaussian distribution of firing rates. This means that the behavior of the ensemble is linear, even though the behavior of the constituent neurons is highly nonlinear. One can then use a Fokker-Planck equation to describe the collective dynamics of the population. The main benefit to these models is that they are well-studied in fields like solid-state physics. However, recent work has shown that the assumption of Gaussian firing rates is not accurate [6]. Firing rates do tend to fall into well-behaved distributions, but not ones that lend themselves to already-developed tools.

For higher coherence within populations (i.e., a non-Gaussian distribution of firing rates), researchers tend to use neural mass models. They assume that nearby neurons in the brain are sufficiently synchronized to model groups of them as a single neuron, with some modifications. Instead of the discrete action potential of a single neuron, neural mass models often have a sigmoidal activation function. They will also simplify the dynamics of the Hodgkin-Huxley model to divide the neural mass's constituent neurons into two subpopulations: an excitatory pool (corresponding to the Na^+ channels in the Hodgkin-Huxley model) and an inhibitory pool (corresponding to the K^+ channels in the Hodgkin-Huxley model).

[3] A full derivation of this model can be found in [9].

[4] One of the classic ways to explain emergence is asking, "Where is the thought in a neuron?"

An example of a neural mass model is the extremely simple Wilson-Cowan model [26]:

$$\tau_x \dot{x} = -xS(C_{xx}x + C_{xy}y + C_{xz}z + P) \tag{1.9}$$
$$\tau_y \dot{y} = -yS(C_{yx}x + C_{yy}y + C_{yz}z + Q) \tag{1.10}$$
$$\tau_z \dot{z} = -zS(C_{zx}x + C_{zy}y + C_{zz}z + R) \tag{1.11}$$

x represents an excitatory process (like the flow of Na^+), and y and z represent inhibitory processes (like the flow of K^+). The time constants τ_i determine the rates of the dynamics of the three processes. It is worth noting that chaotic dynamics can occur when multiple different time scales are present [6]. The coupling strengths C_{ij} represent the connectivity between the three processes, with $C_{ix} \geq 0$ (making x excitatory) and $C_{i\{y,z\}} \leq 0$ (making y inhibitory). P, Q, and R represent the excitability threshold, or the constant external inputs to each process (similar to I_m in eq. (1.7)). The sigmoidal activation function $S(x) = \frac{1}{1+e^{-a(x-\theta)}}$ represents the mass effect of the population of neurons being modeled. This system provides an excellent toy model which reflects meso-scale dynamics accurately, relative to its simplicity.

Macro-scale Models

These models do an accurate job of representing the behavior of small parts of the brain. However, it is not reasonable to carry the assumptions of un- or highly-correlated activity to the large-scale activity of whole-brain dynamics. In order to make these models accurately depict the overall behavior of the brain as a whole, researchers turn to two main techniques: *neural field models* and *neural mass networks*. The first treats the brain as a continuous sheet of cortex, within which activity obeys wave equations. The second represents the brain as a discrete graph of cortices, or a network of coupled oscillators. An example of a neural mass network model is the modified Hindmarsh-Rose model (eqs. (3.1) to (3.3)), which is discussed later.

One of the benefits of a neural mass network model is that its outputs are similar to those of an *electroencephalograph*, or *EEG*. The EEG is a device used to record the electrical activity of the brain. Electrodes are placed in specific areas on the scalp, and then measure changes in voltage from neural masses beneath the skull. Much of the signal is distorted and attenuated by the bone and tissue between the brain and the electrodes, which act like resistors and capacitors. This means that, while the membrane voltage of the neuron changes by millivolts, the EEG reads a signal in the microvolt scale [27]. Additionally, the EEG has relatively low spatial and temporal resolution (16 electrodes for the whole brain, and a sampling rate of 33 ms). However, when properly treated, neural mass models make for effective predictors of the output from EEGs [15, 25]. This is useful, as EEGs are the main tool used to detect and categorize seizures.

1.2.2 Seizure Ætiology

For centuries, and across many cultures, seizures were viewed as holy and mystical events, and those with epilepsy were often considered to be shamans [8, 27]. Seizures are often accompanied by strange visions, sounds, or smells (called *auras*), and sometimes manifest themselves physically in extreme ways. External symptoms can include convulsions of the limbs or the entire body, or a seeming trance. In societies that are unfamiliar with the root causes of seizures, this can be a terrifying and awe-inspiring sight to behold.

In more recent years, researchers have come to define seizures as abnormal, excessive, or overly-synchronized neural activity [4, 27]. It is important to distinguish between seizures and epilepsy, as the two are often conflated. Seizures are an acute event, whereas epilepsy is a chronic condition

of repeated seizures. While classification schemes vary, all center around the division between *generalized* and *focal* seizures.

Generalized seizures involve the entire brain, and start in both hemispheres at the same time, which is why they are often called *primary generalized seizures*. The manifestation of these seizures crosses an entire spectrum. They sometimes hardly present to an external observer, as in the case of the *typical absence seizure*[5], which is nonconvulsive and results in a complete cessation of motor activity for approximately 10 seconds. Patients lose consciousness, but not posture, making it seem to an observer like a trance or simply "spacing out."

On the other side of the range is the *tonic-clonic seizure*, wherein effectively all of a patient's muscles contract at once for around 30 seconds (the tonic phase), and then clench and unclench rapidly, resulting in jerking of the extremities (the clonic phase) for 1 to 2 minutes. After tonic-clonic seizures (in the *postictal* phase), patients often report confusion, muscle soreness, and exhaustion.

Focal seizures start in one part of the brain (the seizure *focus*). They are generally preceded by auras such as a sense of fear, or hearing music, and often manifest as clonic movement of the extremities. In many cases, they secondarily generalize, spreading to the entire brain. This can make focal seizures and primary generalized seizures hard to distinguish, as a focal seizure can generalize rapidly after a brief aura. This can lead to misdiagnoses and improper treatments.

The Epileptor Model

From careful observation, an empirical/phenomenological seizure model called Epileptor was developed [11, 12]. It involves two fast processes x_1 and y_1, two *spike-wave event* processes x_2 and y_2, and a slow permittivity variable z. Its guiding equations are:

$$\dot{x}_1 = y_1 - f_1(x_1, x_2) - z + I_{\text{rest1}} \tag{1.12}$$
$$\dot{y}_1 = y_0 - 5x_1^2 - y_1 \tag{1.13}$$
$$\dot{z} = \frac{1}{\tau_0}(4(x_1 - x_0) - z) \tag{1.14}$$
$$\dot{x}_2 = -y_2 + x_2 - x_2^3 + I_{\text{rest2}} + 0.002g(x_1) - 0.3(z - 3.5) \tag{1.15}$$
$$\dot{y}_2 = \frac{1}{\tau_2}(-y_2 + f_2(x_1, x_2)) \tag{1.16}$$

where

$$g(x_1) = \int_{t_0}^{t} e^{-\gamma(t-\tau)} x_1(\tau)\, \mathrm{d}\tau \tag{1.17}$$
$$f_1(x_1, x_2) = \begin{cases} x_1^3 - 3x_1^2 & x_1 < 0 \\ x_1\big(x_2 - 0.6(z-4)^2\big) & x_1 \geq 0 \end{cases} \tag{1.18}$$
$$f_2(x_1, x_2) = \begin{cases} 0 & x_2 < -0.25 \\ 6(x_2 + 0.25) & x_2 \geq -0.25 \end{cases} \tag{1.19}$$

The required parameters have the following values: $x_0 = -1.6$, $y_0 = 1$, $\tau_0 = 2857$, $\tau_1 = 1$, $\tau_2 = 10$, $I_{\text{rest1}} = 3.1$, $I_{\text{rest2}} = 0.45$, $\gamma = 0.01$. A feature to note is that $\tau_0 \gg \tau_2 \gg \tau_1$. As previously mentioned, these vastly different time scales allow for chaotic dynamics to occur, and contribute to the nonlinearity of the system.

[5]Since a lot of early epilepsy research was performed in French-speaking regions, "absence" is pronounced æbˈsɑns.

While the Epileptor model is highly accurate, and is currently being used to develop patient-specific models and treatments, its main issue is that it is purely phenomenological. The variables and parameters in the model directly correspond to physical processes, but the model's development was largely empirical, and not fully rooted in theory [12]. This means that it can be a helpful tool in treating symptoms, but is not necessarily as valuable for determining root causes.

Chapter 2

Literature Review

It is important to get a sense of how the area of nonlinear dynamics has been applied to neuroscience. One of the most powerful tools for describing the qualitative behavior of a nonlinear system is *bifurcation analysis*, determining how the number and stability of fixed points and limit cycles changes as parameters of a model change [24].

2.1 Bifurcation Analyses of Seizure Models

Analyses of the dynamics of brain models can provide an understanding of the mechanisms underlying a wide variety of brain behaviors. Multistability and bifurcations can be interpreted as being at the center of many different states, from seizures to switching from syncopated to anti-syncopated finger tapping [4–6, 12, 21, 26]. With that in mind, it is worthwhile to look at some examples of bifurcation analyses of neural models.

2.1.1 The Wilson-Cowan Model

One of the simplest models which lends itself to bifurcation analysis is the Wilson-Cowan model (eqs. (1.9) to (1.11)). Traces of x over time look remarkably like the output from an EEG scan. Figure 2.1 shows a simulation of the Wilson-Cowan model with the parameters[1]:

Add in changin z

$$C = \begin{bmatrix} 23 & -15 & -10 \\ 35 & 0 & 0 \\ 10 & 0 & 0 \end{bmatrix}, \quad \begin{bmatrix} P \\ Q \\ R \end{bmatrix} = \begin{bmatrix} 3 \\ -5 \\ -5 \end{bmatrix}, \quad \tau = \begin{bmatrix} 0.015 \\ 0.013 \\ 0.267 \end{bmatrix} \tag{2.1}$$

These results show a stereotypical spike-wave event, represented to a high degree of accuracy.

The main challenge to performing bifurcation analysis on this type of system is two-fold. The first aspect is that there are 15 parameters to vary. This makes bifurcation analysis exceedingly difficult, as all 15 dimensions and their relationships to each other must be analyzed. This is closely related to the second aspect of the challenge this model provides: the variables in this model are abstracted from their physical/physiological meanings. For example, because the coupling strengths do not correspond directly to any measurable values, it is hard to gain actionable semantic knowledge from analysis of their effects on the system [12].

[1] Parameters taken from [26], table 1. Note that the values in rows 3(g),3(i) and 3(j),3(l) should be switched.

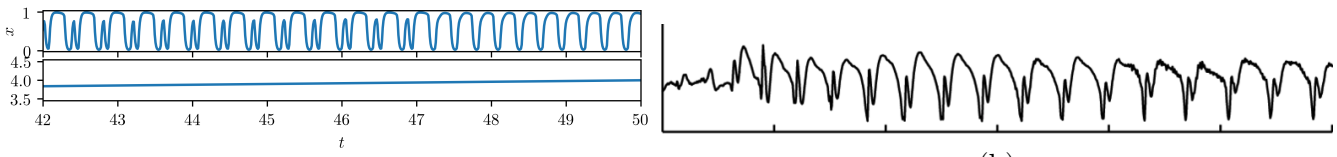

(a) (b)

Figure 2.1: A comparison of a simulation of the Wilson-Cowan system and an actual EEG trace of spike-wave event. (a) The output of a simulation of the Wilson-Cowan model (eqs. (1.9) to (1.11)) using parameters from [26]. A 4th-order Runge-Kutta solver ($\mathrm{d}t = 0.01$, $t_{\max} = 1000$) was run on the Wilson-Cowan model with parameters shown in eq. (2.1). (b) An EEG trace of a spike-wave event, often characteristic of absence seizures. Taken and modified from [16].

2.1.2 The Epileptor Model

In the Epileptor model (eqs. (1.12) to (1.17), (1.18) and (1.19)), bifurcations depending on the slow permittivity variable z (which acts as a parameter) determine whether the brain is behaving normally, or having a seizure [12]. Particularly, as is the case with many similar models, normal steady-state brain function corresponds to a stable fixed point, while seizure-like events are on stable limit cycles. This raises the question: what kinds of bifurcations occur during the transition from healthy brain activity to seizures and back?

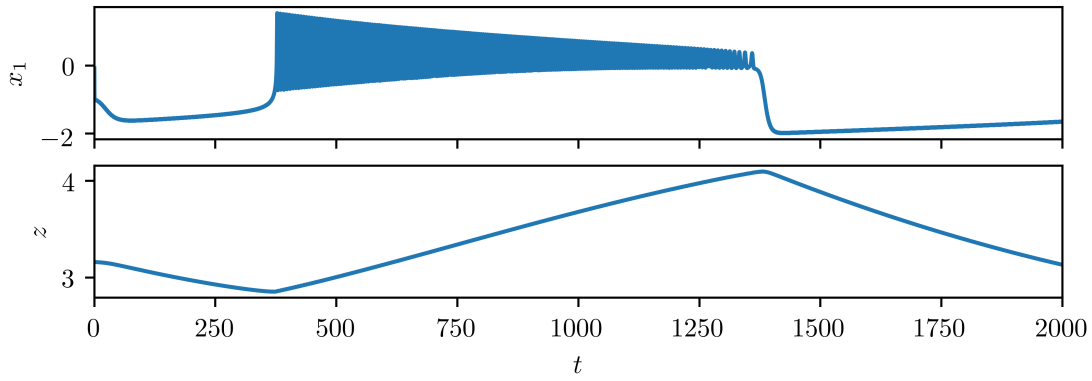

Figure 2.2: A simulation of the Epileptor model showing the observable x_1 and the slow-changing permittivity variable z, using a 4th-order Runge-Kutta solver ($\mathrm{d}t = 0.01$, $t_{\max} = 2000$) and the parameters listed in section 1.2.2. The brain is exhibiting healthy behavior for $t \in (0, 375) = h_1$, then rapidly jumps into a seizure-like behavior. It stays in this state for $t \in (375, 1360) = s$, until it returns to a healthy fixed point for $t \in (1360, 2000) = h_2$. Note the DC shift, wherein $x_1(s) > x_1(h_1) \approx x_1(h_2)$.

To discuss the dynamics of Epileptor in general, we will use the stereotypical behavior displayed in fig. 2.2. An important aspect of epileptor to note is that x_1 is the closest variable to an observable quantity, but it still does not resemble an EEG trace without some post-processing. Particularly, x_1 would look a lot more like the output from an EEG if put through a high-pass filter. However, there is an invertible map directly between x_1 and the readings from an EEG, so the results can be treated as the same [12].

During seizure onset at $t = 375$, the stable fixed point of healthy activity disappears, replaced

by a stable limit cycle. This indicates that the system undergoes either a Hopf or a saddle-node bifurcation. A hint towards the type of bifurcation involved is that seizures occur suddenly [27]. This means that the amplitude of oscillation does not steadily increase from 0, meaning that a supercritical Hopf bifurcation can be ruled out [24]. Additionally, the DC shift at $t = 375$, which does appear in experiment, indicates that the bifurcation can not be a subcritical Hopf. This leaves only a saddle-node bifurcation for the transition into a seizure [12].

As the seizure ends at $t = 1360$, the model returns from a limit cycle to a fixed point with another DC shift. This indicates that the bifurcation is either a fold bifurcation or a homoclinic bifurcation. One important point of note is that the frequency of oscillation decreases as the seizure approaches offset, which matches with experiment.

Ask Danfort about Scheffer

2.1.3 Neural Field Model

If there's enough time (which seems unlikely) [5].

This.

2.2 Chimera States in the Brain

[3, 10, 21]

Chapter 3

Methods

3.1 Model

An example of a neural mass network is the modified Hindmarsh-Rose model [21].

$$\dot{x}_j = y_j - x^3 + bx_j^2 + I_j - z_j - \frac{\alpha}{n'_j}\sum_{k=1}^{N} G'_{jk}\Theta(x_k) - \frac{\beta}{n''_j}\sum_{k=1}^{N} G'_{jk}\Theta(x_k) \tag{3.1}$$

$$\dot{y}_j = 1 - 5x_j^2 - y_j \tag{3.2}$$

$$\dot{z}_j = \mu(s(x_j - x_{\text{rest}}) - z_j) \tag{3.3}$$

where

$$\Theta(x_k) = \frac{x_j - x_{\text{rev}}}{1 + e^{-\lambda(x_k - \theta)}} \tag{3.4}$$

In this model, x_j is the membrane potential of the jth neural mass, y_j is from the fast processes

Chapter 4

Results

We now investigate three aspects of the results of this work. First, we compare the output from the model to real-world data, on a qualitative level. We then discuss the region of parameter space for which the model produces aphysical results. Finally, we draw connections between chimera states in the model and their physiological analogues.

4.1 Model Quality

4.2 Aphysical Region

4.3 Chimera states

Chapter 5

Conclusion

This is the conclusion!

List of Figures

Bibliography

[1] Daniel M. Abrams and Steven H. Strogatz. "Chimera States for Coupled Oscillators". In: *Physical Review Letters* 93.17 (Oct. 2004). DOI: 10.1103/physrevlett.93.174102. URL: https://doi.org/10.1103/physrevlett.93.174102.

[2] Daniel M. Abrams et al. "Solvable Model for Chimera States of Coupled Oscillators". In: *Physical Review Letters* 101.8 (Aug. 2008). DOI: 10.1103/physrevlett.101.084103. URL: https://doi.org/10.1103/physrevlett.101.084103.

[3] Ralph G. Andrzejak et al. "All together now: Analogies between chimera state collapses and epileptic seizures". In: *Scientific Reports* 6.1 (Mar. 2016). DOI: 10.1038/srep23000. URL: https://doi.org/10.1038/srep23000.

[4] Gerold Baier et al. "The importance of modeling epileptic seizure dynamics as spatio-temporal patterns". In: *Frontiers in Physiology* 3 (2012). DOI: 10.3389/fphys.2012.00281. URL: https://doi.org/10.3389/fphys.2012.00281.

[5] M. Breakspear et al. "A Unifying Explanation of Primary Generalized Seizures Through Nonlinear Brain Modeling and Bifurcation Analysis". In: *Cerebral Cortex* 16.9 (Nov. 2005), pp. 1296–1313. DOI: 10.1093/cercor/bhj072. URL: https://doi.org/10.1093/cercor/bhj072.

[6] Michael Breakspear. "Dynamic models of large-scale brain activity". In: *Nature Neuroscience* 20.3 (Mar. 2017), pp. 340–352. DOI: 10.1038/nn.4497. URL: https://doi.org/10.1038/nn.4497.

[7] Gustavo Deco et al. "The Dynamic Brain: From Spiking Neurons to Neural Masses and Cortical Fields". In: *PLoS Computational Biology* 4.8 (Aug. 2008). Ed. by Olaf Sporns, e1000092. DOI: 10.1371/journal.pcbi.1000092. URL: https://doi.org/10.1371/journal.pcbi.1000092.

[8] A. Fadiman. *The Spirit Catches You and You Fall Down: A Hmong Child, Her American Doctors, and the Collision of Two Cultures*. FSG Classics. Farrar, Straus and Giroux, 1998. ISBN: 9781429931113. URL: https://books.google.com/books?id=DUHAXXvSUeYC.

[9] P. Graben et al. *Lectures in Supercomputational Neuroscience: Dynamics in Complex Brain Networks*. Understanding Complex Systems. Springer Berlin Heidelberg, 2007. ISBN: 9783540731597. URL: https://books.google.com/books?id=GW36HNEs4ucC.

[10] Johanne Hizanidis et al. "Chimera-like States in Modular Neural Networks". In: *Scientific Reports* 6.1 (Jan. 2016). DOI: 10.1038/srep19845. URL: https://doi.org/10.1038/srep19845.

[11] V.K. Jirsa et al. "The Virtual Epileptic Patient: Individualized whole-brain models of epilepsy spread". In: *NeuroImage* 145 (Jan. 2017), pp. 377–388. DOI: 10.1016/j.neuroimage.2016.04.049. URL: https://doi.org/10.1016/j.neuroimage.2016.04.049.

[12] Viktor K. Jirsa et al. "On the nature of seizure dynamics". In: *Brain* 137.8 (June 2014), pp. 2210–2230. DOI: 10.1093/brain/awu133. URL: https://doi.org/10.1093/brain/awu133.

[13] Nikita Kruk, Yuri Maistrenko, and Heinz Koeppl. "Self-propelled chimeras". In: *Physical Review E* 98.3 (Sept. 2018). DOI: 10.1103/physreve.98.032219. URL: https://doi.org/10.1103/physreve.98.032219.

[14] Yoshiki Kuramoto and Dorjsuren Battogtokh. "Coexistence of Coherence and Incoherence in Nonlocally Coupled Phase Oscillators". In: *arXiv e-prints*, cond-mat/0210694 (Oct. 2002), cond–mat/0210694. arXiv: cond-mat/0210694 [cond-mat.stat-mech].

[15] Lutz Leistritz et al. "Coupled oscillators for modeling and analysis of EEG/MEG oscillations". In: *Biomedizinische Technik/Biomedical Engineering* 52.1 (Feb. 2007), pp. 83–89. DOI: 10.1515/bmt.2007.016. URL: https://doi.org/10.1515/bmt.2007.016.

[16] Frank Marten et al. "Onset of polyspike complexes in a mean-field model of human electroencephalography and its application to absence epilepsy". In: *Philosophical Transactions of the Royal Society A: Mathematical, Physical and Engineering Sciences* 367.1891 (Mar. 2009), pp. 1145–1161. DOI: 10.1098/rsta.2008.0255. URL: https://doi.org/10.1098/rsta.2008.0255.

[17] E. A. Martens et al. "Chimera states in mechanical oscillator networks". In: *Proceedings of the National Academy of Sciences* 110.26 (June 2013), pp. 10563–10567. DOI: 10.1073/pnas.1302880110. URL: https://doi.org/10.1073/pnas.1302880110.

[18] Mark J Panaggio and Daniel M Abrams. "Chimera states: coexistence of coherence and incoherence in networks of coupled oscillators". In: *Nonlinearity* 28.3 (Feb. 2015), R67–R87. DOI: 10.1088/0951-7715/28/3/r67. URL: https://doi.org/10.1088/0951-7715/28/3/r67.

[19] James Pantaleone. "Synchronization of metronomes". In: *American Journal of Physics* 70.10 (Oct. 2002), pp. 992–1000. DOI: 10.1119/1.1501118. URL: https://doi.org/10.1119/1.1501118.

[20] Jonatan Peña Ramirez et al. "The sympathy of two pendulum clocks: beyond Huygens' observations". In: *Scientific Reports* 6.1 (Mar. 2016). DOI: 10.1038/srep23580. URL: https://doi.org/10.1038/srep23580.

[21] M.S. Santos et al. "Chimera-like states in a neuronal network model of the cat brain". In: *Chaos, Solitons & Fractals* 101 (Aug. 2017), pp. 86–91. DOI: 10.1016/j.chaos.2017.05.028. URL: https://doi.org/10.1016/j.chaos.2017.05.028.

[22] M.S. Santos et al. "Recurrence quantification analysis of chimera states". In: *Physics Letters A* 379.37 (Oct. 2015), pp. 2188–2192. DOI: 10.1016/j.physleta.2015.07.029. URL: https://doi.org/10.1016/j.physleta.2015.07.029.

[23] Murray Shanahan. "Metastable chimera states in community-structured oscillator networks". In: *Chaos: An Interdisciplinary Journal of Nonlinear Science* 20.1 (Mar. 2010), p. 013108. DOI: 10.1063/1.3305451. URL: https://doi.org/10.1063/1.3305451.

[24] Steven H. Strogatz. *Nonlinear Dynamics and Chaos: With Applications to Physics, Biology, Chemistry, and Engineering*. 1st ed. Westview Press, 2015. This book is essentially the bible of nonlinear dynamics. While it does not cover epilepsy except to briefly mention it as a topic beyond the frontier of the field, I would not be able to understand anything else I have been reading without this book.

[25] Peter Neal Taylor et al. "Towards a large-scale model of patient-specific epileptic spike-wave discharges". In: *Biological Cybernetics* 107.1 (Nov. 2012), pp. 83–94. DOI: 10.1007/s00422-012-0534-2. URL: https://doi.org/10.1007/s00422-012-0534-2.

[26] Yujiang Wang et al. "Phase space approach for modeling of epileptic dynamics". In: *Physical Review E* 85.6 (June 2012). DOI: 10.1103/physreve.85.061918. URL: https://doi.org/10.1103/physreve.85.061918.

[27] Gary L. Westbrook. "Principles of Neural Science". In: ed. by Eric R. Kandel et al. Fifth. McGraw Hill Medical, 2013. Chap. 50, pp. 1116–1139.

[28] Jianbo Xie, Edgar Knobloch, and Hsien-Ching Kao. "Multicluster and traveling chimera states in nonlocal phase-coupled oscillators". In: *Physical Review E* 90.2 (Aug. 2014). DOI: 10.1103/physreve.90.022919. URL: https://doi.org/10.1103/physreve.90.022919.